

Integral equation calculations and computer simulations of the static structure and ionic transport in molten thallium halides

This article has been downloaded from IOPscience. Please scroll down to see the full text article.

1997 J. Phys.: Condens. Matter 9 11061

(<http://iopscience.iop.org/0953-8984/9/50/011>)

View [the table of contents for this issue](#), or go to the [journal homepage](#) for more

Download details:

IP Address: 171.66.16.151

The article was downloaded on 12/05/2010 at 23:17

Please note that [terms and conditions apply](#).

Integral equation calculations and computer simulations of the static structure and ionic transport in molten thallium halides

Ç Tasseven†, O Alcaraz‡, J Trullàs‡, M Silbert‡§ and A Giró‡

† School of Physics, University of East Anglia, Norwich NR4 7TJ, UK

‡ Departament de Física i Enginyeria Nuclear, Campus Nord UPC, Mòdul B4, 08034 Barcelona, Spain

Received 18 December 1996, in final form 4 July 1997

Abstract. We present the first calculations and computer simulations of the static structure and ionic transport properties of molten thallium halides near melting. The calculations have been carried out using the hypernetted-chain theory of liquids (HNC), and for the simulations we have used molecular dynamics (MD). The potentials used for the calculations have the same functional form as the semiempirical potential originally proposed by Vashishta and Rahman (Vashishta P and Rahman A 1978 *Phys. Rev. Lett.* **40** 1337) for studying α -AgI.

The total structure factors obtained from our calculations are in fair qualitative agreement with available neutron scattering data. The local structures of these melts exhibit a behaviour intermediate between those of the noble-metal halides and the alkali halides.

The mean square displacements, velocity autocorrelation functions and distinct correlation functions confirm further this intermediate behaviour suggesting a rather complicated diffusion mechanism where mass and size effects compete strongly. The results for the specific ionic conductivities are in good agreement with experiment if it is assumed that the ions, in their transport, have an integer charge of magnitude $|Z| = 1$, rather than the magnitude of the effective charges used in the potentials.

1. Introduction

This paper is concerned with integral equation calculations and computer simulation studies of the static structure and ionic transport in molten thallium halides (TlX; X = Cl, Br, I) near the melting point. They are, as far as we are aware, the first calculations for these properties of molten TlX to be presented in the literature.

To this end we have used potentials which have the same functional form as those used to study the molten silver and copper halides [1–6]. These were originally proposed by Vashishta and Rahman [7] for studying the β -to- α transition in AgI. Unlike the case for those systems, which either melt from a superionic phase (AgI, CuBr, CuI) or exhibit strong premelting phenomena (CuCl, AgCl, AgBr), there is no clear justification for the use of these potentials in the case of the molten TlX compounds. However, we take the view that these are semiempirical potentials which can be used in the case of the molten thallium halides for the reasons given below.

The molten TlX compounds exhibit several features which distinguish them from the alkali halides, and have always been banded together with the noble-metal halides [8].

§ On study leave from the School of Physics, University of East Anglia at Norwich, UK.

Nagasaka and Kojima [9] have modelled interactions between ions with a potential which assumes charge transfer (from anion to cation) in the copper, silver and thallium halides. Using those potentials they calculated the ionicity f of the copper, silver and thallium halides. For the copper and silver halides their results are in good agreement with those obtained by Phillips [10]. The values of f obtained for the thallium halides—0.854 (TlCl), 0.829 (TlBr), 0.821 (TlI)—fall in between those for the noble-metal halides and the alkali halides in the Phillips scale [10]. All three TlX compounds have CsCl-type crystal structure near their melting points [11]. All of these systems have relatively high ionic conductivities which increase exponentially as the temperature increases, reaching a value of the order of $\sigma \approx 10^{-3} \Omega^{-1} \text{cm}^{-1}$ at zero pressure, just before melting [12]. This value of σ is much higher than that found for the typical alkali halides, but smaller than that for the noble-metal halides. The TlX compounds also have relatively large dielectric constants [13]. This is important to ionic transport because the larger the dielectric constant of an ionic crystal, the lower the energy of formation of lattice defects. Experiments at atmospheric pressure have indicated that the defects in the crystal structure of TlBr [14] and TlCl [15] consist primarily of Schottky defects.

There is very little in the way of experimental information on the molten TlX compounds. Most relevant to this work are the neutron scattering experiments carried out, near the melting point, by Satow *et al* [16]. Our results reproduce their results qualitatively and, hence, give us confidence in the credibility of the other results presented below.

In the following section we present briefly our parametrization of the potentials, as well as minimal information on the solution of the hypernetted-chain (HNC) integral equation theory of liquids and the molecular dynamics (MD) code used in our work. In section 3 we present our results. These are followed by a few relevant conclusions.

2. Formalism

2.1. The potentials

As indicated in the introduction, we have used in our calculations the functional form of the potential originally proposed by Vashishta and Rahman, namely

$$\phi_{\alpha\beta}(r) = \frac{H_{\alpha\beta}}{r^{\eta_{\alpha\beta}}} + \frac{Z_{\alpha}Z_{\beta}e^2}{r} - \frac{P_{\alpha\beta}}{r^4} - \frac{C_{\alpha\beta}}{r^6} \quad (\alpha, \beta = +, -). \quad (2.1)$$

Before we move on to the parametrization of the coefficients in equation (2.1), the following two comments are in order. First, we also attempted to use the potentials given by Mayer [17] for TlX, but the HNC calculations did not converge to a solution for the structure when used in conjunction with the appropriate thermodynamic information—temperature T and density ρ —near the melting point (as given in table 2 later) even when using partial charges. In fact, it is now well established that the applicability of the Born–Mayer-type potentials is severely restricted [18]. The *charge-transfer* potentials developed by Nagasaka and Kojima [9], while predicting reasonable values for the ionicity f , reproduce rather poorly the observed values of the cohesive energy of the TlX crystals. Moreover their predicted potential wells are too deep to be of use for liquid-state calculations. Second, and this is particularly relevant for solid-state calculations, the TlX compounds fail to satisfy the Cauchy relation between the elastic constants, which rules out the use of pair potentials. In fact, for TlX c_{12} is about twice the size of c_{44} [19]. Nonetheless, we submit that our semiempirical potentials remain a useful tool in liquid-state calculations.

The parametrization of the semiempirical potential used in this work, equation (2.1), follows the prescription suggested by Rahman and Vashishta for AgI [20]. However, it is

Table 1. Effective pair potential parameters for TlCl, TlBr and TlI. The units of length are Å and the units of energy are $e^2 \text{Å}^{-1} = 14.399 \text{ eV}$.

$\phi_{\alpha\beta}$	$\eta_{\alpha\beta}$	$H_{\alpha\beta}$	$P_{\alpha\beta}$	$C_{\alpha\beta}$
TlCl ($ Z = 0.68$)				
Tl-Tl	7	15.03	0	0
Cl-Cl	7	133.42	1.60	5.8
Tl-Cl	7	48.75	0.80	0
TlBr ($ Z = 0.70$)				
Tl-Tl	6	9.58	0	0
Br-Br	6	62.25	2.19	9.1
Tl-Br	6	26.26	1.10	0
TlI ($ Z = 0.65$)				
Tl-Tl	5	3.20	0	0
I-I	9	4719.76	3.08	19.0
Tl-I	7	97.85	1.54	0

possible to obtain different sets of parameters which satisfy their prescription. Of these we have chosen that set which, used in conjunction with MD simulations, shows that the system has just melted at the experimental temperature and density. The parameters used in our potentials are shown in table 1. A few comments are in order. In the choice of the inverse-power potentials we have been guided by the values of the isothermal compressibility K_T [17]. Since we were unable to find in the literature a value of K_T for molten TlI, we estimated its value to be $K_T = 10^{-10} \text{ m}^2 \text{ N}^{-1}$. The values of the effective charges found in the literature ($|Z| = 0.8-0.97$), and used in solid-state calculations [9, 21, 22], are higher than those used in our potentials (table 1). However, the values for the ionicity of TlX suggest that the effective charges should be nearer to those used in our calculation for molten AgCl and AgBr ($|Z| = 0.68$ and 0.66 respectively) [4].

Figures 1(a), 1(b) and 1(c) show the potentials used in our calculations for molten TlCl, TlBr and TlI respectively. The differences between $\phi_{\text{TlTi}}(r)$ and $\phi_{\text{XX}}(r)$ at small values of r are due to the difference in size between cations and anions. The minimum in $\phi_{\text{TlX}}(r)$ occurs at 2.48, 2.88, and 3.22 Å for TlBr, TlCl and TlI respectively. These distances are smaller than the cation-anion distances calculated in the solid state, $d_{\text{TlX}} \cong 3.44, 3.32$ and 3.64 Å respectively.

2.2. The HNC theory of liquids and MD simulations

We evaluated the pair distribution functions $g_{\alpha\beta}(r)$ and the partial structure factors $S_{\alpha\beta}(k)$ using both the HNC approximation and MD simulations [23]. From the partial structure factors we reconstructed, using the appropriate neutron scattering lengths b_α , the total structure factor $S_T(k)$ in order to make a direct comparison with the experimental results.

We obtained numerical solutions for the HNC for the pair potentials given in equation (2.1), at temperature T and density ρ , using a method originally due to Gillan [24]. All of the calculations were carried out using $M = 1024$ mesh points.

For our MD simulations we used a set of $N = 512$ ions ($N/2$ anions and $N/2$ cations) placed in a cubic box whose side L is defined by the density ρ , with periodic boundary conditions at temperature T . The procedures used in our simulation code are described

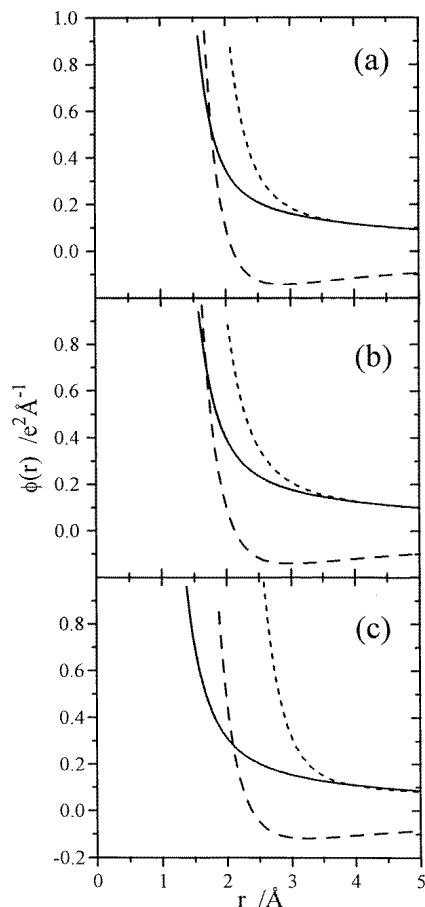


Figure 1. Effective pairwise-additive potentials for molten TlX (X = Cl, Br, I), equation (2.1), in units of $e^2 \text{ \AA}^{-1} = 14.399 \text{ eV}$, with the parametrization given in table 1. (a) TlCl. (b) TlBr. (c) TlI. Solid line: $\phi_{\text{TlI}}(r)$; broken line (long dashes): $\phi_{\text{TlX}}(r)$; broken line (short dashes): $\phi_{\text{XX}}(r)$.

elsewhere and we specifically refer readers to references [4] and [6] for further details (see also reference [25]).

The structural properties studied in this work are the pair distribution functions $g_{\alpha\beta}(r)$ and the partial structure factors $S_{\alpha\beta}(k)$. The latter were calculated *directly* from the density fluctuations [6]. We show the results for $g_{\alpha\beta}(r)$ and $S_{\alpha\beta}(k)$ in the next section.

We also evaluated the mean square displacements $\langle r_\alpha^2(t) \rangle$ ($\alpha = +, -$), and the normalized velocity autocorrelation functions (vacf) $C_\alpha(t)$. We have also evaluated the normalized charge-current-density autocorrelation function $C^Z(t)$, and the normalized distinct correlation function $\delta(t)$ [26].

We have evaluated both the diffusion coefficients D_α and the specific ionic conductivity σ . For the first we used both the Einstein relation and the Kubo formula [27]. For σ we also used the corresponding Kubo formula [27] and the Einstein-like relation discussed by Trullàs and Padró [26]. Results for D_α and σ , also presented in the next section, are normally averages of those obtained from using the two approaches.

Table 2. Input thermodynamic data used in the HNC calculations and MD simulations. ρ is the density, in \AA^{-3} ; T is the temperature, in K. We also include, for comparison, the melting temperature, T_m , also in K.

Input data	TlCl	TlBr	TlI
ρ	0.0271 ^a	0.0246 ^a	0.0210 ^c
T ^b	823	843	833
T_m ^a	702	732	713

^a Reference [27].

^b Reference [16].

^c Estimated (see the text).

It is also possible to use the distinct correlation function to define uniquely the coefficient Δ [26] which measures the deviation of σ from the Nernst–Einstein relation [27]. Our results for Δ are also discussed in the next section.

3. Results

3.1. Liquid structure

We carried out HNC calculations and MD simulations of the liquid structure of TlX at the temperatures quoted by Satow *et al* [16] for their neutron diffraction experiments. The input thermodynamic data are given in table 2. The densities for molten TlCl and TlBr are available in the literature [28], but the value of the density of TlI given in table 2 was estimated. At this estimated density, and for the potentials used in this work, the MD simulations show that the system is a liquid at the given temperature.

The results of our calculations for the pair distribution functions $g_{\alpha\beta}(r)$ are shown in figure 2. We see from the figure that, for values of r beyond the first peak, the HNC results are in good agreement with the MD simulations. The main differences lie in the rather broad first peak of the pair distribution functions of like ions, which also exhibit a shoulder on the high- r side. In the HNC results for the distribution functions of like ions the height of the first peak is always lower, and ‘flatter’, and their positions always at smaller values of r than the MD values. The positions of the first peak of $g_{\alpha\beta}(r)$, $r_{\alpha\beta}^{\max}$, are given in table 3. The $g_{\alpha\beta}(r)$ display more charge penetration and less charge cancellation than the alkali halides, but less than in the molten noble-metal halides—a sign that these systems represent a case intermediate between the two. The behaviour of the first peak, in our view, points to shortcomings in the HNC theory. Similar types of shoulder have been found for molten CsI [29] and RbCl [30], and predicted for AgCl [31], near melting and at normal pressure. However, Ross and Rogers have shown for CsI that, under pressure, this shoulder resolves into a second peak in $g_{\text{CsCs}}(r)$ [29]. Given the results for molten CsI under pressure we conjecture that, likewise, the shoulder for molten TlX is likely to resolve into a second peak if subjected to pressure on account of having the same structure in the solid phase.

We now turn to the coordination numbers $n_{\alpha\beta}$. For the solid, $n_{\text{TlX}} = 8$ and, assuming that the liquid near melting retains the local structure of the solid, we should expect that on average this would be the case for the thallium halides. However, Satow *et al* [16] in the analyses of their experimental data suggest that $n_{\text{TlX}} \cong 6$ and they concluded that, on melting, TlX has a local structure similar to that of, say, molten NaCl. The method of isomorphous substitution in molten salts used by Satow *et al* to obtain $r_{\text{XX}}^{\max}/r_{\text{TlX}}^{\max}$ and hence infer n_{TlX} is suspect and, in fairness, these authors acknowledge that much. Moreover,

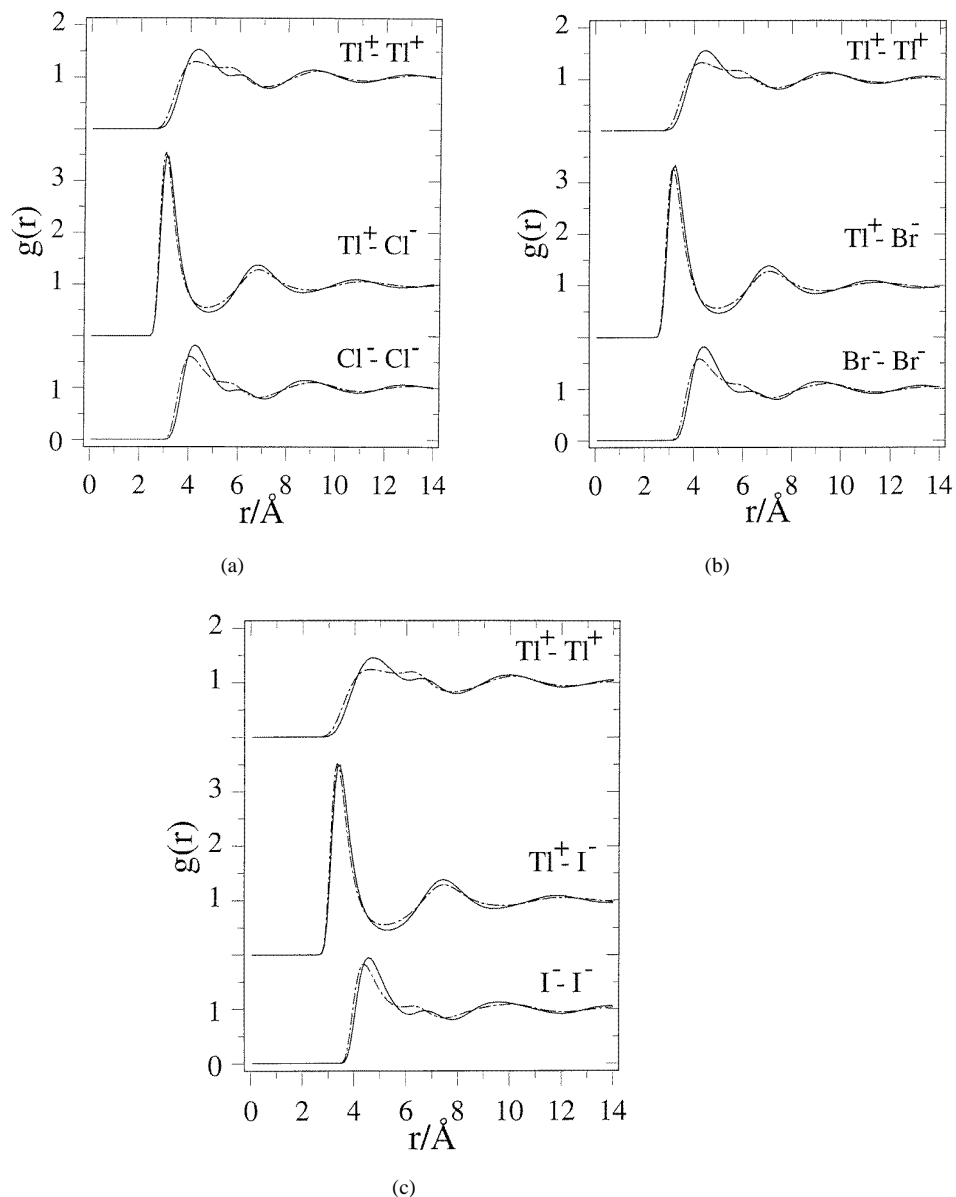


Figure 2. MD (solid lines) and HNC (dash-dotted lines) results for the pair distribution functions $g_{\alpha\beta}(r)$ of molten TlX (X = Cl, Br, I) at the temperatures and densities given in table 2. (a) $g_{\alpha\beta}(r)$ for molten TlCl. (b) $g_{\alpha\beta}(r)$ for molten TlBr. (c) $g_{\alpha\beta}(r)$ for molten TlI.

it is difficult to come to a conclusion based only on the coordination number of unlike ions. Hence, we decided to carefully analyse $n_{\alpha\beta}$. There is another reason for carefully analysing $n_{\alpha\beta}$: whereas the molten alkali halides retain, on average, the same structure of the crystalline solid, AgBr and AgCl change, on melting, from a rock-salt to a zinc-blende-like structure. The results for AgBr and AgCl were found experimentally by Keen *et al* [32], and confirmed by the *ab initio* simulations of Wilson *et al* [31], and our own

Table 3. Structural parameters, coordination numbers, and ionic transport properties of the molten thallium halides.

Parameters		TlCl	TlBr	TlI
$r_{\text{TlI}}^{\text{max}}/\text{\AA}$	MD	4.3	4.5	4.8
	HNC	4.2	4.3	4.6
$r_{\text{XX}}^{\text{max}}/\text{\AA}$	MD	4.3	4.4	4.5
	HNC	4.1	4.3	4.4
$r_{\text{TlX}}^{\text{max}}/\text{\AA}$	MD	3.1	3.2	3.4
	HNC	3.05	3.2	3.3
$n_{\text{TlI}}^{\text{IV}}$	MD	17.0	16.9	17.8
$n_{\text{XX}}^{\text{IV}}$	MD	16.5	16.7	16.8
$n_{\text{TlX}}^{\text{IV}}$	MD	6.3	6.4	6.3
$n_{\text{TlI}}^{\text{V}}$	MD	19.8	20.2	20.9
n_{XX}^{V}	MD	19.5	19.3	19.2
$n_{\text{TlX}}^{\text{V}}$	MD	6.8	6.9	6.9
$D/(10^{-5} \text{ cm}^2 \text{ s}^{-1})$				
D_{Tl}		2.3	2.1	1.9
D_{X}		2.1	1.9	1.7
$\sigma/(\Omega^{-1} \text{ cm}^{-1})$				
$\sigma(Z_{\text{eff}})$		0.6	0.5	0.2
$\sigma(Z = 1)$		1.2	1.0	0.6
σ (experiment) ^a		1.52	1.07	0.64
$\Delta(N = 216)$		0.09	0.05	0.28
$\Delta(N = 512)$		0.19	0.27	0.24

^a Reference [28].

calculations [4].

There are five different methods for evaluating the coordination numbers [33]. However, we only report the MD results obtained using methods iv and v; these are listed in table 3. Those evaluated using the HNC are available on request. We note, in passing, that it was not possible to evaluate n_{TlI} and n_{II} for molten TlI, using the HNC, because of the asymmetric behaviour of the like-pair distribution functions. We recall that method iv evaluates the area of $r^2 g_{\alpha\beta}(r)$ up to its first minimum, whereas method v integrates up to the first minimum of $g_{\alpha\beta}(r)$. We find that, in both cases, $n_{\text{TlX}} \cong 6-7$, whereas $n_{\text{TlI}} \approx n_{\text{XX}} \approx 17-19$. On the basis of these results we conclude that, contrary to the suggestion of Satow *et al*, the TlX compounds retain, on melting, the same local CsCl-like structure that they have in the solid. We base our conclusion on the following points. (i) Although the value of the average coordination number of unlike ions is slightly below the value for the crystal, similar features have been noted in most of the systems for which there are MD results [34]. (ii) More importantly, the first shell of like ions has the 12 + 6 arrangement in the solid CsCl structure, which merges into the shouldered first peak of the like-pair distribution functions giving a commensurate value for the average coordination number. On the other hand, the first coordination shell for solid NaCl of like ions contains twelve ions and is followed by a second coordination shell of unlike ions containing eight ions and a second shell of like ions containing six ions. If the local structure of molten TlX was more like

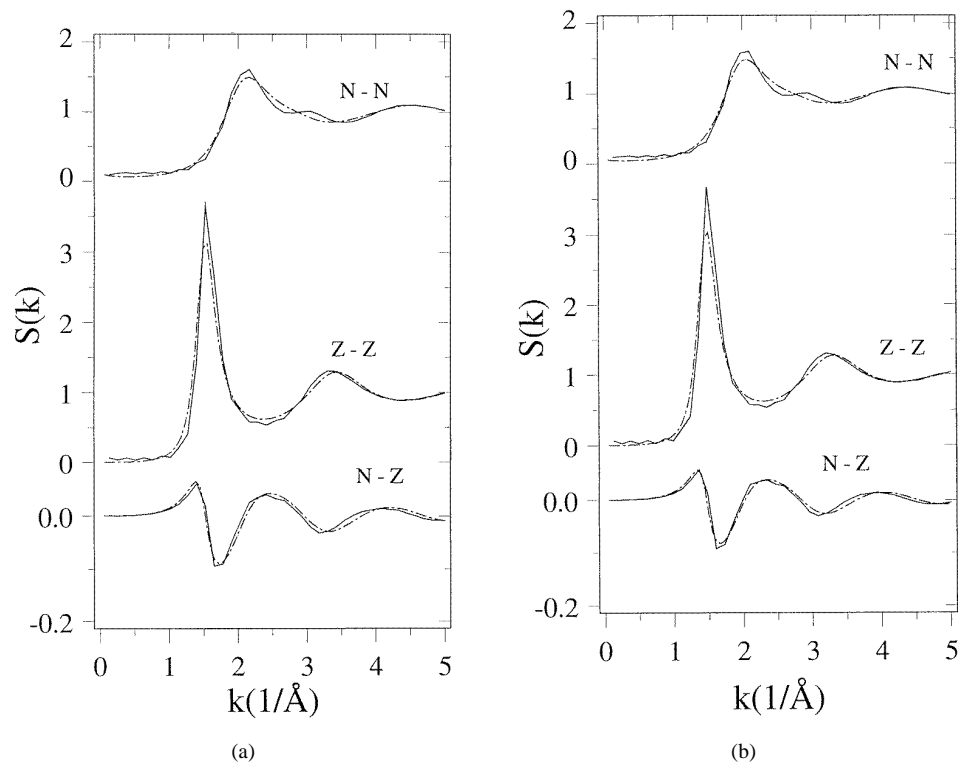


Figure 3. MD (solid lines) and HNC (dash-dotted lines) results for the Bhatia–Thornton partial structure factors of molten TlX at the temperatures and densities given in table 2. Please note the different scale used for $S_{NZ}(k)$. (a) $S_{\alpha\beta}(k)$ for molten TlCl. (b) $S_{\alpha\beta}(k)$ for molten TlBr. (c) $S_{\alpha\beta}(k)$ for molten TlI.

that of NaCl, then there would be some sort of feature, however weak, in $g_{\text{TlX}}(r)$ at about the same position as the shell containing the eight unlike ions; such a feature is not present in $g_{\text{TlX}}(r)$.

We now turn to the partial structure factors. Figure 3 shows the MD and HNC results for the Bhatia–Thornton partial structure factors [22] of molten TlX. The Ashcroft–Langreth partials are not shown but are available on request. Except for the shoulder following the principal peak of $S_{NN}(k)$, the HNC calculations and MD simulations are in reasonably good agreement, particularly if we take into account that the finiteness of the simulation box renders meaningless the simulation of the structure for values of $k \leq 4\pi/L$, and also is subject to fluctuations errors. Notice also that the first peak of $S_{NN}(k)$ is at almost the same position as the principal peak in the total structure factor $S_T(k)$ shown in figure 4. The principal peak of $S_{NN}(k)$ is also at the same position as a shoulder in the Ashcroft–Langreth partial structure factors of anions and the second peak of the partial structure factors of the Tl ions. Hence, these features in the Ashcroft–Langreth partials and the total structure factor can be attributed to density fluctuations. The charge–charge partial structure factor $S_{ZZ}(k)$ is almost typical of an ionic system, but exhibits more oscillations than $S_{ZZ}(k)$ for the alkali halides, reflecting the partial ionicity built into the potentials. Note that the first peak of the simulated $S_{ZZ}(k)$ is higher than that calculated with the HNC, suggesting a higher degree of Coulomb ordering in the former. Finally we note that the coupling between charge

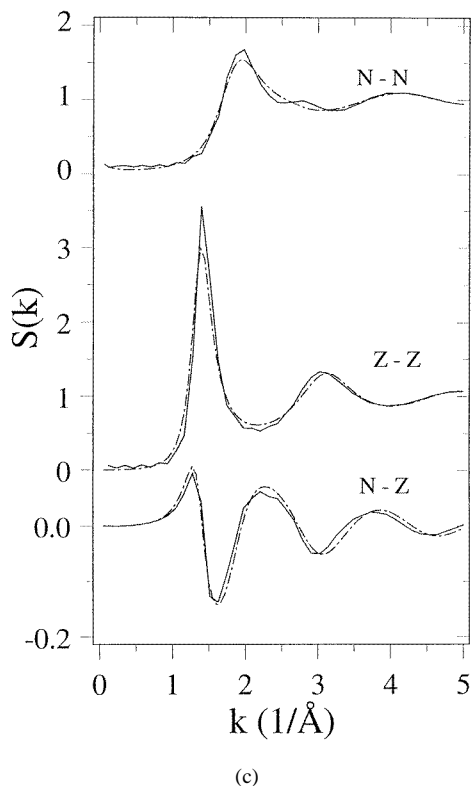


Figure 3. (Continued)

and particle fluctuations, as given by $S_{ZN}(k)$, is not negligible when compared with the same property for the alkali halides. Figure 4—for which we have used a different scale for $S_{ZN}(k)$ to that for the other partials—exhibits oscillations which are not present in the simple molten salts.

Figure 4 compares our MD and HNC results with the experimental total structure factors of molten TlX. The values of the neutron scattering lengths used in our work, in fm (10^{-15} m), are [35]: $b_{\text{Tl}} = 8.776$, $b_{\text{Cl}} = 9.577$, $b_{\text{Br}} = 6.795$ and $b_{\text{I}} = 5.28$. There is a fair qualitative agreement between our results and the neutron scattering data. As noted above, both the position and the height of the principal peak of $S_T(k)$, and to some extent also the other peaks, are dominated by $S_{NN}(k)$. This suggests that the main features of the experimental total structure factor are due to short-range topological order. Only the shoulder, which appears on the low- k side of the principal peak in the total structure factor of TlI (faintly in the experimental and MD $S_T(k)$, more noticeably in the HNC results), is at the same position as the principal peak of the charge fluctuation partial structure factor $S_{ZZ}(k)$ and has its origin in charge ordering. For TlCl the position of the experimental first peak is shifted towards slightly larger values of k ; this shift is smaller for TlBr and TlI. The height of the first peak is bounded by our MD simulations, which always give higher values, and the HNC results, which are always slightly lower. The MD simulations exhibit a similar type of shoulder on the high- k side of the principal peak of $S_T(k)$, albeit in a different position and with different heights to those exhibited by experiment; this shoulder does not show up in the HNC simulations.

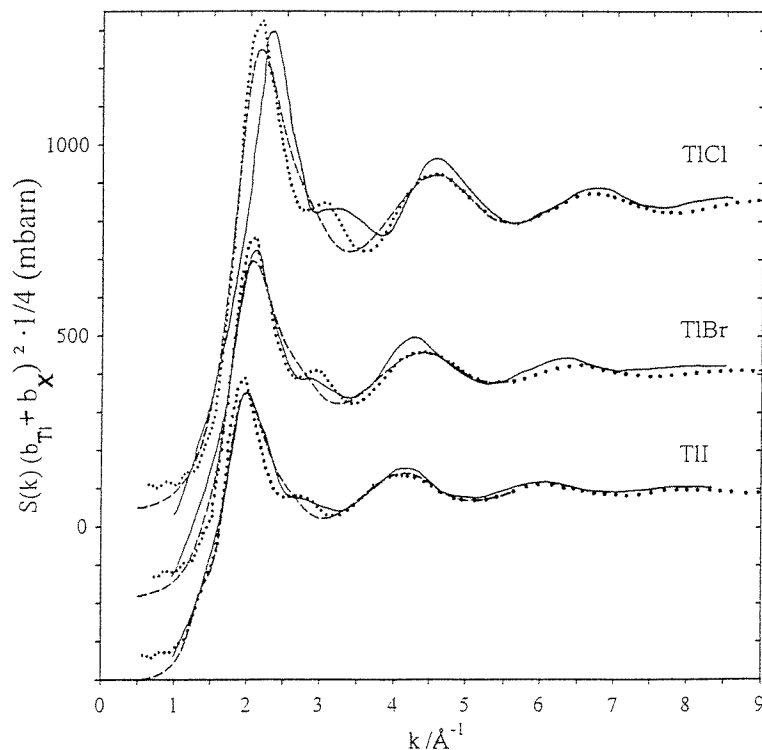


Figure 4. Total structure factors $S_T(k)$ of molten TlX ($X = \text{Cl}, \text{Br}, \text{I}$) at the temperatures and densities given in table 2. Solid line: neutron scattering data [16]; dotted line: MD simulations; broken line: HNC results.

3.2. Ionic transport

Figure 5 shows the mean square displacements $\langle r_\alpha^2(t) \rangle$ ($\alpha = +, -$) for TlX. They suggest some unusual features of the diffusion mechanism of these ions, at both intermediate and long times, which we discuss below in conjunction with our results for the velocity autocorrelation functions (vacf), $C_\alpha(t)$, which are shown in figure 6.

The features which require some explanation are the differences in the behaviour of $\langle r_\alpha^2(t) \rangle$ at intermediate times, $t \approx 0.4\text{--}0.6$ ps, and for long times. In order to try to understand these results it is useful to recall briefly both our interpretation for the mechanism of diffusion in the noble-metal halide melts [4, 6], and that given for the molten alkali halides [27].

We suggested that, in the noble-metal halides, the anions—the *larger* ions—experience a ‘rattling’ motion in the cage formed by the neighbouring anions, with the cations only playing the role of ‘holding’ the cage as they move through it in their largely diffusive behaviour. This picture is moderated in the case of the molten AgCl and AgBr because the size difference between cations and anions is not as large as in the other cases. The alkali halides exhibit a ‘rattling’ motion of the *lighter* ions—irrespective of their sign—in the relatively long-lived cage formed by their heavier neighbours.

The picture that we suggest for the TlX melts is that they exhibit a mix of the two mechanisms. Of course ours is a somewhat schematic pictorial description in need of both experimental and theoretical corroborating evidence.

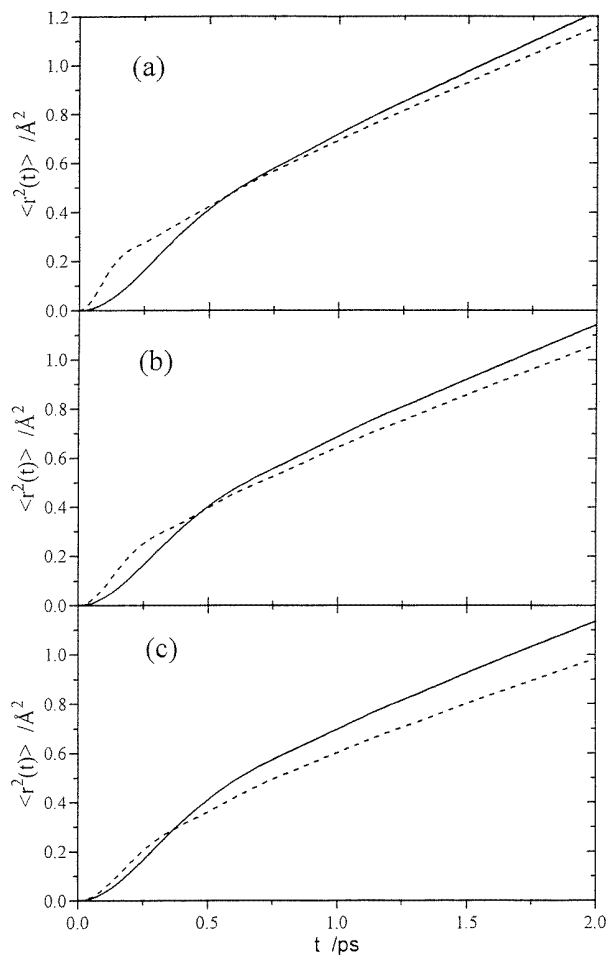


Figure 5. MD results for the mean square displacements, $\langle r_\alpha^2(t) \rangle$, of molten TlX (X = Cl, Br, I) at the temperatures and densities given in table 2. (a) $\langle r_\alpha^2(t) \rangle$ for molten TlCl. Solid line: $\langle r_{\text{Tl}}^2(t) \rangle$; broken line: $\langle r_{\text{Cl}}^2(t) \rangle$. (b) $\langle r_\alpha^2(t) \rangle$ for molten TlBr. Solid line: $\langle r_{\text{Tl}}^2(t) \rangle$; broken line: $\langle r_{\text{Br}}^2(t) \rangle$. (c) $\langle r_\alpha^2(t) \rangle$ for molten TlI. Solid line: $\langle r_{\text{Tl}}^2(t) \rangle$; broken line: $\langle r_{\text{I}}^2(t) \rangle$.

We suggest that, for $t \approx 0.4\text{--}0.6$ ps, there is a complicated behaviour of a cage of anions (the lighter ions in all of the three cases studied here) around another anion, and another—fuzzier—cage of cations around the same anion. Within the latter the anions oscillate strongly, and the strength of the oscillations in the vacf increases with increasing mass difference between anions and cations. This shows up as a deeper backscattering, as shown in figure 6, for TlCl with $m_{\text{Tl}}/m_{\text{Cl}} = 5.8$. Hence the diffusion mechanism for the anions, at this stage, is more like that for the molten alkali halides. As the anion breaks through this cage there is a change of slope in $\langle r_\alpha^2(t) \rangle$ that is more pronounced for molten TlI. The anion then ‘sees’ the cage of the like anions which it finds more difficult to break through, so in the diffusive regime it is still slower than the cations. Thus the behaviour of an anion as it goes through the second cage is more like that found for the molten noble-metal halides.

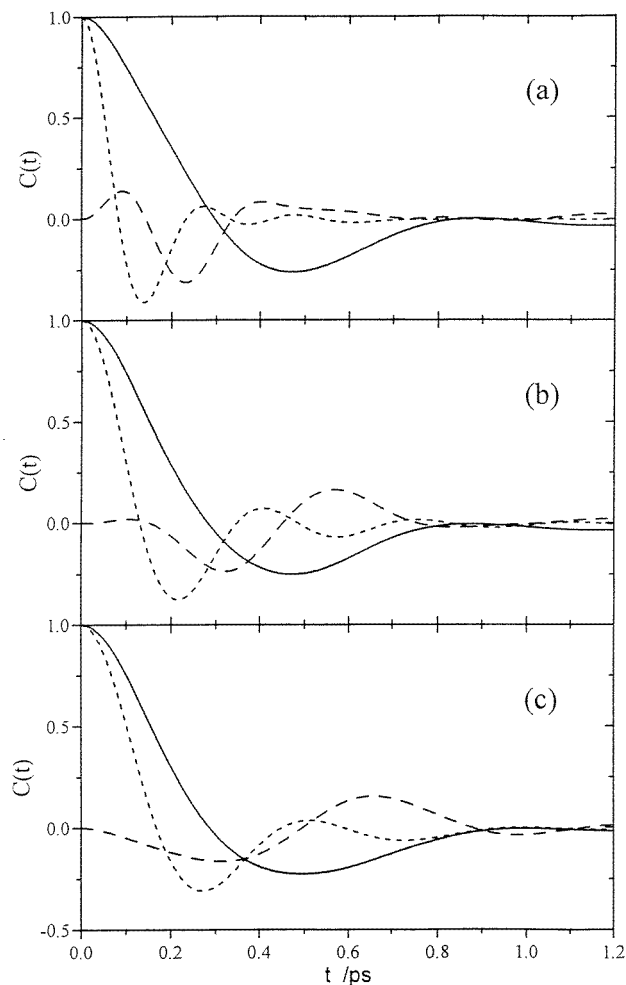


Figure 6. MD results for the normalized velocity autocorrelation functions, $C_{\alpha}(t)$, and normalized distinct velocity correlation function, $\delta(t)$, of molten TlX ($X = \text{Cl}, \text{Br}, \text{I}$) at the temperatures and densities given in table 2. (a) $C_{\alpha}(t)$ and $\delta(t)$ for molten TlCl. Solid line: $C_{\text{Tl}}(t)$; broken line (short dashes): $C_{\text{Cl}}(t)$; broken line (long dashes): $\delta(t)$. (b) $C_{\alpha}(t)$ and $\delta(t)$ for molten TlBr. Solid line: $C_{\text{Tl}}(t)$; broken line (short dashes): $C_{\text{Br}}(t)$; broken line (long dashes): $\delta(t)$. (c) $C_{\alpha}(t)$ and $\delta(t)$ for molten TlI. Solid line: $C_{\text{Tl}}(t)$; broken line (short dashes): $C_{\text{I}}(t)$; broken line (long dashes): $\delta(t)$.

The cations exhibit weaker backscatterings which are rather similar for the three systems. As the cations break up their cage they show a change of slope in $\langle r_{\text{Tl}}^2(t) \rangle$ that becomes more pronounced with size difference, namely in TlI. However, the cations find it easier to break through the cage of anions because they are the smaller ions. Hence in the diffusive regime they remain the more mobile, but only slightly so.

We note that there appears to be a mass effect in the short-time behaviour of the distinct correlation functions. $\delta(t)$ is initially positive when the mass ratio is larger, as in TlCl, but it is initially negative when the mass ratio decreases significantly, as in TlI. There also appears to be a correspondence between the strength of the oscillations in $\delta(t)$ and the depth

of the first minimum in $C_X(t)$. This is an empirical observation based on all of the systems that we have studied, including in this work [4, 6]. We believe that it may be related to the interplay between mass and size difference between cations and anions. However, we have not been able, so far, to formulate this observation quantitatively.

We now turn to the properties characterizing ionic transport, namely diffusion coefficients and the specific ionic conductivity. The results for both D_α and σ are given in table 3. The results for D_α confirm the trends expected from the $\langle r_\alpha^2(t) \rangle$ results, with the diffusion constants for the cations only slightly larger than those for the anions. There are no experimental results of D_α , to our knowledge, available in the literature for the molten TlX. However, we submit that, on the basis of the values obtained for the specific ionic conductivity discussed below, the values that we obtain for the diffusion constants are fairly reliable and can be used with confidence.

We actually carried out two different calculations for σ : one using the same effective charge as was used for the potentials, and the other using a charge $Z = 1$. It is possible to produce arguments supporting either case. For the former there is the argument of self-consistency in the calculations. For the latter, which we favour, we argue that, whereas in their interactions the ions ‘see’ effective charges, in their transport the ions carry with them their full complement of electrons. The results that we obtain in the two cases are shown in table 3 where we also include the experimental data [28]. The results for σ obtained using Z_{eff} are between one third and one half below the experimental data, whereas those obtained with $Z = 1$ are in good agreement with experiment, with the largest difference found for TlCl. The results for σ obtained using $Z = 1$ can go either way when compared to those obtained using Z_{eff} . We have found that the values for σ obtained using $Z = 1$ improve for the silver halides but worsen for the copper halides [6]. We believe that the reason for this may be related to whether or not the parametrization of our potentials encourages a higher mobility in the ions. However, we cannot prove this statement until experimental information on the diffusion coefficients of molten TlX become available. For the TlX melts the calculated conductivity is always below the experimental value which, in turn, suggests that we are underestimating the values of the diffusion constants.

The value of Δ is very sensitive to the numerical evaluation of the integral of the distinct correlation function. We have also found that the value of this integral is sensitive to the number of particles used in the simulations. The results for Δ obtained by using both 216 and the 512 used in this work are shown in table 3. We have also checked how sensitive the value of Δ is, with the cut-off placed at different times for $\delta(t)$, and find that with 512 ions it is much less sensitive than when using 216 ions. Hence we are confident that the value obtained with 512 ions is likely to remain unchanged if the simulation uses a larger set of ions. In fact the values obtained from the simulations with 512 ions show some degree of consistency for the three systems studied which is not found with the smaller set of ions. The values of Δ obtained with the former are all positive. This is an important difference *vis à vis* the noble-metal halides where Δ is always negative and from the case of, say, molten NaCl where Δ is approximately zero. We have also verified that the values for the diffusion constants and the specific ionic conductivity are not sensitive to the number of ions used in our simulations.

Finally we would like to stress that the important quantity here is $\delta(t)$ rather than Δ . The latter measures empirically departures from the Nernst–Einstein relation. However, a value of Δ near zero is not necessarily the signature of a simple molten salt, for in most, if not all, cases this means that the oscillations in $\delta(t)$ tend to cancel. From this point of view an ideal molten salt is one where there are no oscillations in $\delta(t)$, and this does not happen even for the simplest of model molten salts [27].

4. Conclusions

We have presented the results of the first integral equation calculations and molecular dynamics simulations for the molten thallium halides obtained using a semiempirical potential whose functional form was originally proposed by Vashishta and Rahman for studying the properties of α -AgI [7].

The combination of the two approaches made possible the study of the static structure and ionic transport properties for these ionic melts. The results thus obtained are in fair qualitative agreement with the rather scarce experimental information available on these systems. In fact, even some of those which are available are not necessarily too reliable. The neutron scattering experiments were fraught with difficulties both in the preparation of the samples and in the actual measurements on account of the high vapour pressure present in the thallium salts [36]. We hope that the present calculations are sufficiently convincing to motivate new experimental studies of the structure of these systems. Moreover, such studies would be useful to confirm whether our estimated density for molten TlI is sensible.

Although we are confident of the general trends, we want to qualify our picture of the molten thallium halides as cases intermediate between the molten alkali halides and the noble-metal halides. Neither the former nor the latter can be regarded as rigid blocks, as there is a rich variety of behaviour in both classes of system. Nonetheless we submit that given the important qualitative differences between these two classes of molten salts, this grouping makes sense, and places the molten thallium halides in between the two.

The interpretation of the diffusion mechanisms that we are putting forward is in need of independent verification and, at the very least, experimental information on the diffusion constants would be extremely useful. We are confident of the trends shown by our results but, in the end, only experiment can decide.

In spite of our arbitrary choice, it is clear that the semiempirical potentials used in the present study do work. Yet it is not clear why. For instance, there is no justification for dropping the contribution due to the polarization of the Tl^+ ions with, say, $\alpha = 3.5 \text{ \AA}^3$ according to Mayer [17], or equal to 5.2 \AA^3 according to Tessman *et al* [37], given that both of these values are comparable to those of the halides for which we used the values quoted by Mayer [17].

Madden and co-workers have recently suggested that the unusual structural and ionic transport properties of materials which, on electronegativity grounds, might be expected to be ionic can be shown to be a consequence of polarization effects [18, 31, 38]. The thallium halides may prove an important testing ground for the validity of their suggestion.

Acknowledgments

It is a pleasure to thank S Tamaki for correspondence and discussions regarding all aspects of this work. This work was partially supported by the DGICYT of Spain under Grant No PB93-0971-C03. ÇT is grateful to Yildiz Technical University at Istanbul for a scholarship tenable at the University of East Anglia, while MS gratefully acknowledges the support of the Generalitat of Catalonia (Spain).

References

- [1] Stafford A J and Silbert M 1987 *Z. Phys.* B **67** 31
- [2] Shimojo F and Kobayashi M 1991 *J. Phys. Soc. Japan* **60** 3725
- [3] Kobayashi M and Shimojo F 1991 *J. Phys. Soc. Japan* **60** 4076

- [4] Tasseven Ç, Trullàs J, Alcaraz O, Silbert M and Giró A 1996 *J. Chem. Phys.* **106** 7286
- [5] Stafford A J, Silbert M, Trullàs J and Giró A 1990 *J. Phys. C: Solid State Phys.* **2** 6631
- [6] Trullàs J, Giró A and Silbert M 1990 *J. Phys. C: Solid State Phys.* **2** 6643
- [7] Vashishta P and Rahman A 1978 *Phys. Rev. Lett.* **40** 1337
- [8] Tosi M P 1964 *Solid State Physics* vol 16 (New York: Academic) p 1
- [9] Nagasaka S and Kojima T 1987 *J. Phys. Soc. Japan* **56** 671
- [10] Phillips J C 1970 *Rev. Mod. Phys.* **42** 317
- [11] Wyckoff R W G 1965 *Crystal Structures* 2nd edn, vol VI (New York: Wiley)
- [12] Samara G A 1981 *Phys. Rev.* **B 23** 575
- [13] Samara G A 1968 *Phys. Rev.* **165** 575
- [14] Herrman P 1964 *Z. Phys. Chem.* **227** 338
- [15] Friauf R J 1971 *Z. Naturf.* **26** 1210
- [16] Satow W, Uemura O, Hoshino K and Watanabe T 1984 *Phys. Status Solidi a* **85** K5
- [17] Mayer J E 1933 *J. Chem. Phys.* **1** 327
- [18] Madden P A and Wilson M 1996 *Chem. Soc. Rev.* **25** 339
- [19] Gray D E (ed) 1972 *American Institute of Physics Handbook* 3rd edn (New York: McGraw-Hill)
- [20] Rahman A and Vashishta P 1983 *Physics of Superionic Conductors* ed J W Perran (New York: Plenum) p 93
- [21] Cowley E R and Okazaki A 1967 *Proc. R. Soc.* **300** 45
- [22] Haridas C, Sundararajan R and Krishnamurthy N 1988 *Can. J. Phys.* **66** 630
- [23] Rovere M and Tosi M P 1986 *Rep. Prog. Phys.* **49** 1001
- [24] Abernethy G M and Gillan M J 1980 *Mol. Phys.* **39** 839
- [25] Allen M P and Tildesley D J 1987 *Computer Simulation of Liquids* (Oxford: Clarendon)
- [26] Trullàs J and Padró J A 1994 *Phys. Rev.* **E 50** 1162
- [27] Hansen J-P and McDonald I R 1986 *Theory of Simple Liquids* 2nd edn (New York: Academic)
- [28] Janz G J, Dampier F W, Lakshminarayanan G R, Lorenz P K, and Tomkins R P T 1968 *Molten Salts (National Standard Reference Data Series 15)* (Gaithersburg, MD: National Bureau of Standards)
- [29] Ross M and Rogers F J 1985 *Phys. Rev.* **B 31** 1463
- [30] Mitchell E W J, Poncet P F J and Stewart R J 1976 *Phil. Mag.* **34** 721
- [31] Wilson M, Madden P A and Costa-Cabral B J 1996 *J. Phys. Chem.* **100** 1227
- [32] Nield V M, Keen D A, Hayes W and McGreevy R L 1992 *J. Phys.: Condens. Matter* **4** 6703
and see also
Nield V M 1993 *DPhil Thesis* Oxford University
- [33] Waseda Y 1980 *The Structure of Non-Crystalline Materials* (New York: McGraw-Hill)
- [34] Enderby J E and Neilson G W 1980 *Adv. Phys.* **29** 323
- [35] Sears V F 1992 *Neutron News* **3** 26
- [36] Tamaki S 1996 private communication to MS
- [37] Tessman J R, Kahn A H and Shockley W 1953 *Phys. Rev.* **92** 890
- [38] Wilson M and Madden P A 1993 *J. Phys.: Condens. Matter* **5** 2687